Appl. Phys. A 81, 1299–1301 (2005)
DOI: 10.1007/s00339-004-3050-y

Applied Physics A
Materials Science & Processing

M.L. SÁNCHEZ[1,✉]
I. BETANCOURT[2]
R. VALENZUELA[2]
B. HERNANDO[1]

Frequency evolution of the magnetoimpedance effect in stress annealed Co-rich amorphous ribbons

[1] Dpto. de Física, Universidad de Oviedo, Calvo Sotelo s/n, 33007 Oviedo, Spain
[2] Institute for Materials Research, National University of Mexico, P.O. Box 70-360, Mexico D.F. 04510, Mexico

Received: 7 June 2004/Accepted: 20 September 2004
Published online: 18 November 2004 •

ABSTRACT Complex impedance measurements in the 1 kHz–10 MHz frequency range have been performed on CoFeSiB ribbons, subjected to different annealing treatments in order to modify their magnetic properties. The different impedance responses as a function of the applied magnetic field are explained by the magnetization processes that take place in the ribbons at different selected frequencies. In particular, an evolution from domain wall to spin rotation is observed in the 50 kHz–2 MHz frequency range, modulated by the changes introduced by the annealing treatments.

PACS 75.30.Gw; 75.50.Kj; 75.60.Ch; 75.60.Nt; 81.05.Kf

1 Introduction

The magneto impedance (MI) effect is a large change of impedance that occurs in a ferromagnetic material when it is submitted to a magnetic field, and when an ac current is flowing through the sample. This behaviour is due to the skin effect, that at high frequencies (above 10 kHz), changes the current distribution inside the sample. As this skin effect depends on the magnetic properties of the material through the magnetic permeability, it can be understood that it is strongly influenced by magnetic fields, tensile and torsional stresses, annealing treatments, or other factors that change the domain structure and magnetic properties of the material.

The MI effect has been observed in soft magnetic materials of all geometries, ribbon, film or wire shaped amorphous and nanocrystalline materials [1–4]. Attention is paid to materials showing large responses of MI, but since the MI effect presents a large sensitivity to magnetic field, and to tensile or torsion stresses, it can also be used as a research tool for evaluating some magnetic properties of materials, like the anisotropy field, magnetostriction or magnetization processes [5, 6].

Amorphous ribbons show a MI effect, which depends on the magnetic properties of the samples. The saturation magnetostriction coefficient is a key parameter to obtain a large impedance response [7], and it can be controlled by the sample composition. High permeabilities are advisable in order to get good responses as well. A further annealing treatment of the as-quenched ribbons leads to changes in these properties, and enables the tailoring of the MI response. The behaviour of the impedance also gives information about the magnetization processes that take place in the material.

✉ Fax: +34-985103324, E-mail: mlsr@uniovi.es

2 Experimental Techniques

We have employed $Co_{66}Fe_4Si_{12}B_{18}$ alloy ribbons obtained by the melt spinning technique. Samples denoted as “M1” were submitted to an annealing treatment at 400 °C during 1 hour with an applied tensile stress of 350 MPa. Samples assigned as “M2” were stress-annealed at 400 °C with an applied tensile stress of 300 MPa and afterwards they were submitted to a relaxation treatment at 400 °C during 1 hour. The samples have a cross-section of $0.5 \times 0.0198\,mm^2$ and a 10 cm length. The hysteresis loops showed a saturation magnetization of 0.58 T for both samples. The saturation magnetostriction coefficients obtained by the SAMR technique were 3×10^{-7} and 4.1×10^{-7} for the M1 and M2 samples, respectively, which are close to zero values, characteristic of materials with a good MI response.

MI measurements were carried out in a system which includes an HP 4192 A impedance analyzer with a 100 Hz–13 MHz frequency range, and a 300-turn solenoid powered by a dc source allowing dc fields up to 80 Oe.

The samples were carefully clamped and their real and imaginary components of impedance were determined. Frequency was chosen in the range 1 kHz–10 MHz, where magnetization processes by domain wall displacement and magnetization rotation can take place. A solenoid was used to apply a magnetic field up to 20 Oe along the axis of the ribbons.

3 Results and discussion

The complex impedance can be written as $Z = Z' + jZ''$, where $j = (-1)^{1/2}$, where Z' and Z'' are the real and imaginary components of impedance, respectively, directly obtained from the impedance analyzer.

The real part of impedance is related to the sample electrical resistance, and the imaginary component is related to the inductance, and therefore to the magnetic permeability. The dependence of these components with the applied magnetic field in the axial direction has been studied in the samples, for several values of the drive current frequency.

At low frequencies the magnetization processes due to domain wall movements are expected to dominate the response. At a certain value of frequency, the relaxation frequency f_x, the domain walls become unable to follow the driving field, and the dominant magnetization process is the moment rotation. The relaxation frequencies of the ribbons M1 and M2 are 400 and 300 kHz, respectively [8].

The evolution of the MI peaks is evident in Figs. 1 and 2. Figure 1 shows the real and imaginary components of the impedance in the stress annealed sample M1, for three selected values of the frequency. At low frequencies (50 kHz) both components of impedance show three well defined peaks. A central peak, which is related to the domain wall displacements, exhibits a more important contribution in the real part. Two symmetric peaks at around the anisotropy field of the sample have been related to the magnetization processes that take place by moment rotations. These peaks are higher in the imaginary component of impedance.

As the frequency increases (100 kHz), the central peak shows some hysteresis in these samples, due to the hysteretic character of the domain wall displacements, and it decreases its size, although the symmetric peaks at the anisotropy field increases. At a frequency of 2 MHz the domain walls are damped, the central peak has disappeared, and the impedance shows the characteristic two-peak structure.

Figure 2 shows the frequency evolution of the MI real and imaginary components in the M2 sample, that was stress-relaxated before it was stress-annealed. The existence of a central peak is not very clear in the resistance at 50 kHz, in the lower frequency range. At this frequency, only a shoulder appears in the reactance, together with the two peaks close to the anisotropy field. The shoulder is smaller at the frequency

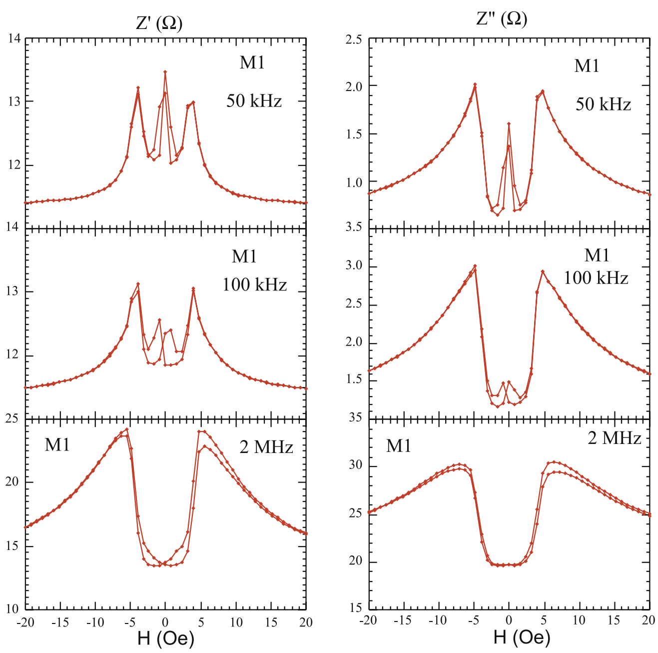

FIGURE 1 Complex impedance of M1 sample (400 °C, 350 MPa) as a function of the increasing and decreasing magnetic field. The *first column* is the real part and the *second* the imaginary part of impedance

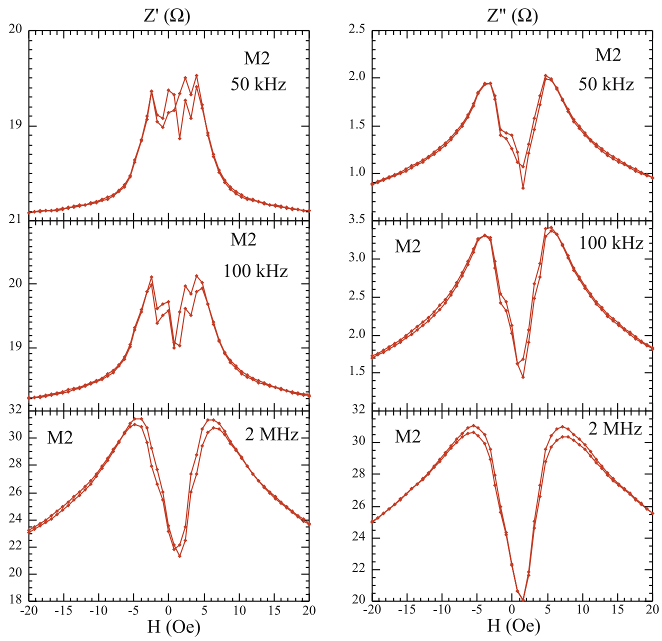

FIGURE 2 Resistance (*first column*) and reactance (*second column*) as a function of the increasing and decreasing magnetic field for the M2 sample (stress-relieved after an annealing treatment) and for three selected values of the drive current frequency

of 100 kHz, and at 2 MHz, only the two-peak structure can be observed in both parts of the complex impedance. This sample shows much less hysteresis than the stress annealed-sample [8], due to a decreased number of the pinning centers, and a better induction of a transversal anisotropy after the stress-relaxation procedure.

At low frequencies the magnetization processes take place by domain wall movement. The reversible bulging of pinned domains is active at low frequencies [9, 10], below the relaxation frequency, f_x, (400 kHz for M1 and 300 kHz for M2), as it can be seen in Figs. 1 and 2 for both samples. The central peak disappears at higher frequencies (2 MHz). The reduction of pinning centres in the M2 sample, due to the previous stress-relief treatment, reduces the central peak in the MI response.

The presence of more than two maxima in MI plots can be attributed to the fact that these measurements were carried at frequencies close to the domain wall relaxation frequency. For very low frequencies (a few decades below f_x), a single peak is observed in impedance measurements in transverse anisotropy wires [11]. This behaviour is associated with the damping of domain wall movements under the dc field [12]. In contrast, at high frequencies (a few decades above f_x), the dominant magnetization process is spin rotation, and a double peak plot appears as a consequence of the increase in spin rotation as the dc field approaches the anisotropy field. At this point, the spin rotation axis change from the transverse to the longitudinal direction.

Our results show, therefore, this transition between domain wall and spin rotation processes; due to its higher relaxation frequency, the central peak in M1 plots is more evident (Fig. 1) and remains at higher frequencies than in M2 plots (Fig. 2). The evolution of the impedance response is more evident in Z'' plots in both cases, probably due to the direct correlation between imaginary impedance and real permeability. The changes observed on Z' exhibit also the effects of the skin depth decrease, since Z' is associated with the resistive part of impedance.

The two-peak structure shows some peaks around the anisotropy field of the samples. The anisotropy field of the samples were obtained from the hysteresis loops, measured by a conventional induction technique. The anisotropy field of the M1 and M2 samples are 5 Oe and 4 Oe respectively. These values correspond to the reactance peaks at low frequencies. The reactance is related to the magnetic permeability, and reflects the magnetic behaviour of the samples. At higher frequencies the peaks of both, resistance and reactance, moved to somewhat higher values, due to the skin effect, that shields the inner part of the ribbons, and has been related to a higher anisotropy of the outer shells of the ribbons [6]. This shift is very small, of no more than 1 Oe.

After performing a stress-annealing treatment, a transverse induced anisotropy is developed in Co-rich amorphous ribbons. This induced anisotropy has three components of different origin: anelastic and plastic anisotropies, and the anisotropy arising from residual internal stresses. The saturation magnetostriction coefficient increases with the annealing treatment. The magnetization processes in this sample (M1) are domain wall displacement and rotations, which are irreversible, producing some hysteretic behavior, as can be seen in Fig. 1, even in the higher frequency range (resistive component, at 2 MHz).

When a further stress-relief is done to the samples (M2), the hysteretic central peaks of the sample M1 disappear, as can be observed in Fig. 2. This treatment results in a decrease in the anisotropy field, decreasing the anelastic component of the anisotropy, as well as the wall pinning centres. The contribution from the reversible magnetization processes is then dominant.

As a conclusion, we have shown the effects of different stress-annealing processes on the impedance response of amorphous CoFeBSi ribbons. By carrying out measurements at frequencies about the domain wall relaxation frequency, it was evident the evolution from the one-peak domain wall damping to the two-peak, change of spin rotation axis processes.

ACKNOWLEDGEMENTS We acknowledge projects MAT–06942, Spain, and IN119603-3 PAPIIT-UNAM, Mexico, for financial support.

REFERENCES

1 L.V. Panina, K. Mohri: Appl. Phys. Lett. **65**, 1189 (1994)
2 F.L.A. Machado, C.S. Martins, S.M. Rezende: Phys. Rev. B **51**, 3926 (1995)
3 K.R. Pirota, L. Kraus, H. Chiriac, M. Knobel: J. Magn. Magn. Mater. **226**, 730 (2001)
4 H.G. Guo, H. Kronmüller, J. Dragon, C. Chen, B.G. Shen: J. Appl. Phys. **84**, 5673 (1998)
5 M. Knobel, C. Gómez-Polo, M. Vázquez: J. Magn. Magn. Mater. **160**, 243 (1996)
6 B. Hernando, M.L. Sánchez, V.M. Prida, M. Tejedor, M. Vázquez: J. Appl. Phys. **90**, 4783 (2001)
7 J.M. Barandiaran, A. Hernando: J.Magn. Magn. Mater. **268**, 309 (2004)
8 V.M. Prida, M.L. Sánchez, B. Hernando, P. Gorria, M. Tejedor, M. Vázquez: Appl. Phys. A **77**, 135 (2003)
9 R. Valenzuela: Phys. B **299**, 280 (2001)
10 I. Betancourt, R. Valenzuela: Appl. Phys. Lett. **83**, 2022 (2003)
11 R. Valenzuela, M. Vazquez, A. Hernando: J. Appl. Phys. **79**, 6549 (1966)
12 K.L. Garcia, R. Valenzuela: IEEE Trans. Mag. **34**, 1162 (1998)